Numerical modelling of primary ship waves in shallow coastal areas using CFD

Ahmet Soydan, Norwegian University of Science and Technology, ahmet.soydan@ntnu.no
Fabian Knoblauch, Norwegian University of Science and Technology, fabian.knoblauch@ntnu.no
Widar Weizhi Wang, Norwegian University of Science and Technology, widar.w.wang@ntnu.no
León-Carlos Dempwolff, Technische Universität Braunschweig, l.dempwolff@tu-braunschweig.de
Nils Goseberg, Technische Universität Braunschweig, n.goseberg@tu-braunschweig.de
Hans Bihs, Norwegian University of Science and Technology, hans.bihs@ntnu.no

INTRODUCTION

Ship generated waves have gained special attention nowadays due to the increasing ship sizes and marine traffic, resulting in higher ship-induced loads in shallow coastal areas. As highlighted by Dempwolff et al. (2022a), the long-period, primary wave system is generated when large-volume ships are traveling in inland waterways, affecting the ecology and the engineering structures. Various numerical methods have been employed to investigate the impact of the ship-generated waves in shallow coastal areas, based on potential flow theory (Yau and Zou, 2010; Gourlay et al., 2015), Reynolds-averaged Navier-Stokes equations (RANSE) (Tezdogan et al., 2016; Terziev et al., 2018) and shallow water equations (SWE) (Lesser et al., 2004; Parnell et al., 2015) as described by Dempwolff et al. (2022a). More recently, Dempwolff et al. (2022b) investigated the ship generated and long-period waves using the open-source SWE solver REEF3D::SFLOW and validated the numerical method. In this work, on the other hand, the high-fidelity hydrodynamic model REEF3D::CFD, accompanied with a fluid-structure interactions (FSI) algorithm, is used to predict the ship-generated wave. The numerical model is validated with the experimental benchmark test carried out by German Federal Waterways Engineering and Research Institute (BAW) in the ship wave basin. Furthermore, this study presents the capability and flexibility of the FSI algorithm for coastal and marine engineering applications.

METHODOLOGY

The ship generated wave is investigated using RANS solver REEF3D::CFD (Bihs et al. 2016) in conjunction with a rigid-body FSI algorithm. For this study, a Post-PANAMAX container vessel with a 1:40 scale is considered. A rectangular numerical wave tank is created to represent the experimental shallow water wave basin, as shown in Figure 1. Numerical beaches, each with a length of 20 m, are applied to all sides of the numerical wave tank to absorb waves generated by the ship. Grid stretching is implemented around the ship and free-surface, as depicted in Figure 1. Two different ship speeds are considered for this study: 8 knots and 14 knots, corresponding to full-scale conditions. Free surface elevation and current velocity data are obtained from the gauges placed in the numerical wave tank, similar to the experimental setup. A direct-forcing immersed boundary approach is employed to model rigid-body motion in the fluid domain. The numerical results obtained by the gauges are compared with experimental data.

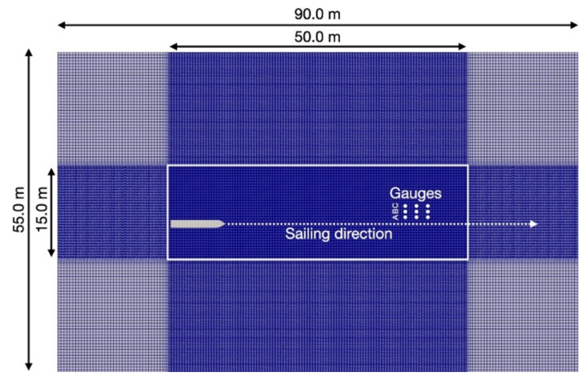

Figure 1 - Numerical wave tank with grids, representing the dimensions and gauges

NUMERICAL MODEL

The open-source RANS solver REEF3D::CFD solves the incompressible continuity and RANS equations in the entire Eulerian domain,

$$\nabla \cdot \boldsymbol{u} = 0$$

$$\frac{\partial \boldsymbol{u}}{\partial t} + \boldsymbol{u} \cdot \nabla \mathbf{u} = -\frac{1}{\rho}\nabla p + \nabla(\nu[\nabla \boldsymbol{u} + \nabla \boldsymbol{u}^T]) + \boldsymbol{g}$$

where $\boldsymbol{u}$ is the velocity vector, ρ is the density of the fluid, p is the pressure, ν is the sum of the kinematic and turbulent viscosity, and $\boldsymbol{g}$ the acceleration vector due to gravity. In the method, the turbulence effect is included by adding turbulent viscosity to the diffusion term using the Boussinesq approximation and a modified $k-\omega$ turbulence model (Bihs et al. 2016). The level set function is used for the transition between air and water phases. The system of equation is solved on a rectilinear staggered grid using finite differences method. For spatial and temporal discretization, high-order schemes are used, such as 5th-order WENO schemes and 3rd-order Runge-Kutta schemes, respectively. The third-order accurate Total Variation Diminishing (TVD) Runge-Kutta scheme is applied for the solution of the time derivatives as well as for free-surface convection.

A direct forcing immersed boundary approach is implemented in REEF3D::CFD (Martin et al., 2021) to take into account the rigid body in fluid domain. A forcing term f is added in the momentum equation to represent the solid velocity field.

$$\frac{\partial \boldsymbol{u}}{\partial t} + \boldsymbol{u} \cdot \nabla \boldsymbol{u} = -\frac{1}{\rho}\nabla p + \boldsymbol{g} + \boldsymbol{f}$$

The forcing term is calculated as:

$$\boldsymbol{f}^{n+1} = H \cdot \left(\frac{\boldsymbol{P}(u^*) - \boldsymbol{u}^*}{\alpha_k \, \Delta t} \right)$$

where H is the smoothed Heaviside function constructed with a level set function. $\boldsymbol{P}(\boldsymbol{u}^*)$ and $\boldsymbol{u}^*$ represent the rigid body velocity and fluid velocity in each Runge-Kutta sub-step, respectively. α_k is a Runge-Kutta coefficient and Δt is time-step. The intermediate solid body velocity field is defined as:

$$\boldsymbol{P}(u^*) = \dot{\boldsymbol{x}} + \boldsymbol{\omega} \times \boldsymbol{r}$$

where $\dot{\boldsymbol{x}}$ is the translational rigid-body velocity vector, $\boldsymbol{\omega}$ is the angular rigid body-velocity vector and $\boldsymbol{r}$ is the distance vector to the rigid body's centre of gravity. The rigid-body in fluid domain is represented with an STL file geometry and the body forces and momenta are calculated by integrating the fluid properties over the discrete rigid-body surface.

DISCUSSION

The time-histories of free surface elevation for a ship speed of 8 knots, obtained from gauge C, is shown in Figure 2 alongside the experimental result. The preliminary numerical result exhibits a slight over-prediction, but, in general, it shows good agreement with experimental data. A more comprehensive validation on the primary wave height and return current velocities will be performed for both ship speed of 8 and 14 knot.

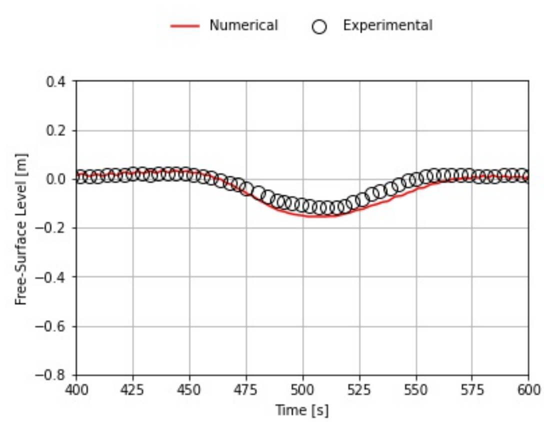

Figure 2 - Time histories of free-surface wave elevation obtained for V=8 knots

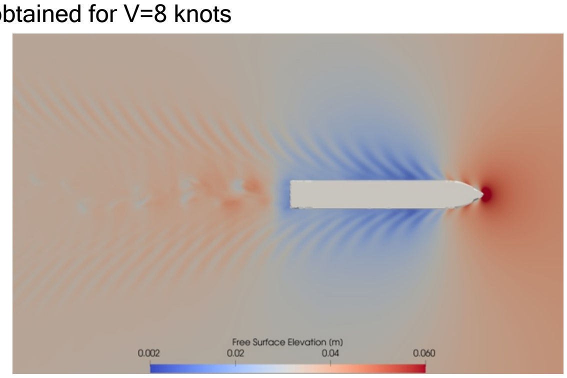

Figure 3 - Free surface elevation elevation contour for V=14 knots, showing the primary waves

ACKNOWLEDGEMENTS

The authors are grateful for the grants provided by the Research Council of Norway under the IPIRIS project (no. 308843). Some simulations were performed on resources provided by Sigma2 - the National Infrastructure for High Performance Computing and Data Storage in Norway.

REFERENCES

Dempwolff, L. C., Melling, G., Windt, C., Lojek, O., Martin, T., Holzwarth, I., Bihs, H. & Goseberg, N. (2022). Loads and effects of ship-generated, drawdown waves in confined waterways-A review of current knowledge and methods. Journal of Coastal and Hydraulic Structures, 2, 46-46.

Yao, J.x. and Zou, Z.j. (2010). Calculation of ship squat in restricted waterways by using a 3d panel method. Journal of Hydrodynamics, 22(S1), 472-477.

Gourlay, T., Ha, J.H., Mucha, P., Uliczka, K. et al. (2015). Sinkage and trim of modern container ships in shallow water, In: the proceedings of the 22nd Australasian Coasts & 15th Ports Conference 2015, Auckland, New Zealand, 344.

Martin, T., Kamath, A., Bihs, H. (2021). Accurate modeling of the interaction of constrained floating structures and complex free surfaces using a new quasistatic mooring model. International Journal for Numerical Methods in Fluids, Vol. 93, Nr. 2.

Tezdogan, T., Incecik, A. and Turan, O. (2016). A numerical investigation of the squat and resistance of ships advancing through a canal using CFD. Journal of Marine Science and Technology, 21(1), 86-101.

Terziev, M., Tezdogan, T., Oguz, E., Gourlay, T., Demirel, Y.K. and Incecik, A. (2018). Numerical investigation of the behaviour and performance of ships advancing through restricted shallow waters. Journal of Fluids and Structures, 76, 185-215.

Lesser, G.R., Roelvink, J.A., van Kester, J. and Stelling, G.S. (2004). Development and validation of a three-dimensional morphological model. Coastal Engineering, 51(8-9), 883-915.

Parnell, K.E., Soomere, T., Zaggia, L., Rodin, A., Lorenzetti, G., Rapaglia, J. and Scarpa, G.M. (2015). Ship-induced solitary riemann waves of depression in venice lagoon. Physics Letters A, 379(6), 555-559.

Dempwolff, L. C., Windt, C., Melling, G., Martin, T., Bihs, H., Holzwarth, I., & Goseberg, N. (2022). The influence of the hull representation for modelling of primary ship waves with a shallow-water equation solver. Ocean Engineering, 266, 113163.

Bihs, H., Kamath, A., Chella, M. A., Aggarwal, A., & Arntsen, Ø. A. (2016). A new level set numerical wave tank with improved density interpolation for complex wave hydrodynamics. Computers & Fluids, 140, 191-208.